JOURNAL OF SPACECRAFT AND ROCKETS
Vol. 44, No. 2, March–April 2007

Determination of Atmospheric Densities from Reentry Flight Data

P. zur Nieden* and H. Olivier†
RWTH Aachen University, 52062 Aachen, Germany

DOI: 10.2514/1.19338

Two methods to infer freestream densities from in-flight measurements of pitot pressure and flight velocity during reentry are presented that focus on the minimization of uncertainties due to high-temperature real-gas effects and atmospheric density fluctuation. A numerical approach leads to a curve-fit function that yields the ratio of the pitot to the dynamic pressure p_{t2}/q_∞ for velocities between 0.5 and 10 km/s and altitudes up to 90 km. An analytically derived correlation is also provided. Both techniques account for equilibrium real-gas effects thus achieving very high accuracies. Independently of potential atmospheric fluctuation, remaining errors are less than 1% for almost the entire spectrum and less than 0.3% for typical lifting reentry.

Nomenclature

A_{ref}	=	reference area
a	=	speed of sound, constant
c_L	=	lift coefficient
c_p	=	specific heat capacity
e	=	specific internal energy
e_f, e_q	=	relative error of f and q
f	=	curve-fit function
h	=	specific enthalpy
Ma	=	Mach number
m	=	mass of flight vehicle
p	=	pressure
q	=	dynamic pressure
T	=	temperature
u, V	=	velocity
γ	=	ratio of specific heats
ρ	=	density

Subscripts

$t2$	=	stagnation-point value
2	=	postshock value
$2E$	=	postshock value for equilibrium flow
∞	=	freestream value

I. Introduction

THE development of future space transportation systems requires the improvement of physical modeling by means of aerothermodynamic design tools, that is, wind-tunnel testing, computational fluid dynamics (CFD), and flight testing. Insufficient capability of ground-based simulation facilities due to poor flow similarity is one of the driving factors for flight testing. Numerical methods have improved significantly over recent years. However, there is a strong need for validation of these tools by means of data acquired in authentic flight environment. For the evaluation of the data obtained during flight tests, however, accurate knowledge of the freestream parameters is crucial. Ambient density is a primary variable in the evaluation of flight dynamics and fluid dynamics phenomena of reentry spacecraft. A major problem, though, originates from the fact that atmospheric fluctuations may cause unpredictable deviations from standard-atmospheric models. These deviations may reach extremes as large as 80% over vertical distances of a few kilometers [1]. Figure 1 shows the deviations measured during three flights of the space shuttle as compared to the U.S. standard atmosphere.

To overcome the difficulties due to density fluctuations as described above, the prevailing atmospheric density at any time can be inferred from pitot-pressure data obtained through in situ pressure measurements. Commonly, a calorically perfect gas model is used for this calculation inevitably leading to significant uncertainties that arise from the real-gas effects associated with the hypersonic flight regime [2,3]. Established methods that would allow for these high-temperature effects are complex numerical computations that require time-consuming data reduction procedures resulting in a high amount of time and effort.

The present paper focuses on the minimization of uncertainties as well as complexity and thus expenditure of application time employing a pressure-based air-data system (ADS) to deduce the freestream density. It provides a method derived from numerical computation and a second approach based on analytical considerations, both allowing for real-gas effects and thus leading to distinctly improved results as compared to conventional techniques. Their important advantage is the combination of this high accuracy with the simplicity of their application. It makes the two methods presented highly effective and results in very short computing times, which renders them suitable for online data reduction during reentry, providing precise data, for example, for flight control loops.

II. Determination of Freestream Density by Means of a Novel Approach

A. Review of Pressure-Based Air-Data Systems

By sampling the pressure distribution at the nose of a craft during flight, it is possible to infer air-data parameters. A pressure model describing the relationship between air data and measured nose pressures is needed to estimate air-data parameters. For perfect gas, the appropriate relation can be expressed in an analytically closed form. However, in the high-enthalpy flight regime associated with the reentry of space vehicles, real-gas effects cause an increase in the pitot pressure to be measured [2]. To date, most of the air-data systems are based on the assumption of perfect-gas behavior to avoid complex data reduction procedures. However, this inevitably leads to reduced accuracies. In this case, substituting the freestream static pressure

Received 2 January 2006; revision received 21 July 2006; accepted for publication 11 August 2006.

*Research Engineer, Institute of Aeronautics and Space Technology, Templergraben 55.

†Professor, Shock Wave Laboratory, Templergraben 55. Member AIAA.

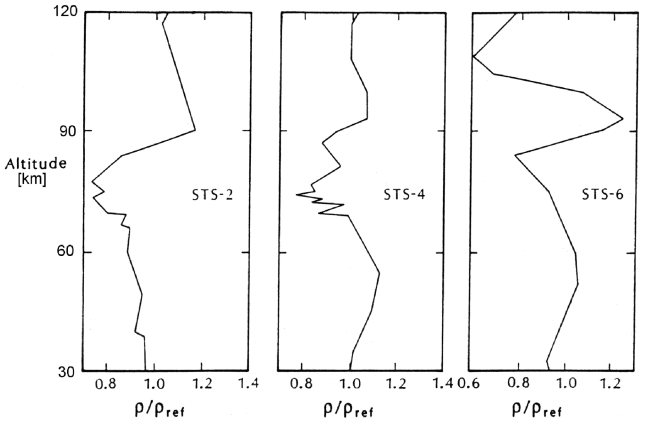

Fig. 1 Shuttle-derived densities compared to the 1962 U.S. standard atmosphere [7].

$$p_\infty = \frac{2q_\infty}{\gamma Ma_\infty^2} \tag{1}$$

into the *Rayleigh pitot tube formula* [4] yields an exact relation for the ratio of the pitot pressure to the freestream dynamic pressure in the supersonic flow of a calorically perfect gas,

$$\frac{p_{t2}}{q_\infty} = \frac{2}{\gamma Ma_\infty^2}\left(\frac{(\gamma+1)^2 Ma_\infty^2}{4\gamma Ma_\infty^2 - 2(\gamma-1)}\right)^{\frac{\gamma}{\gamma-1}}\left(\frac{1-\gamma+2\gamma Ma_\infty^2}{\gamma+1}\right) \tag{2}$$

For high freestream Mach numbers ($Ma_\infty^2 \gg 1$), the limit $Ma_\infty \to \infty$ can be used as an approximation,

$$\frac{p_{t2}}{q_\infty} \approx \left[\frac{(\gamma+1)^2}{4\gamma}\right]^{\frac{\gamma}{\gamma-1}}\left[\frac{4}{\gamma+1}\right] \tag{3}$$

Using the hypersonic approximation of Eq. (3), the freestream density can be determined from pitot-pressure measurements during atmospheric flight if the flight velocity is known, for example, via GPS (global positioning system). For air ($\gamma = 1.4$), Eq. (3) yields $p_{t2}/q_\infty = 1.839$.

Müller-Eigner et al. [3] give another approximate relation that can be used to evaluate the freestream density for $Ma_\infty > 5$:

$$\frac{p_{t2}}{q_\infty} \approx \frac{\gamma+3}{\gamma+1} \tag{4}$$

Equation (4) is derived on the basis of incompressible flow between shock and stagnation point, that is, $p_{t2} = p_2 + q_2$ and with p_2 and q_2 calculated with hypersonic normal shock approximations ($Ma \gg 1$). For air ($\gamma = 1.4$), Eq. (4) yields $p_{t2}/q_\infty = 1.833$.

In high-enthalpy flows, real-gas effects occur as shown in Fig. 2. According to Koppenwallner and Müller-Eigner [2], the increase in pitot pressure due to real-gas effects is on the order of magnitude of 5% and has to be accounted for. Enzian et al. [1] state that "the atmospheric density has to be known with an accuracy of 1 to 3% in order to estimate real-gas effects." This demonstrates the need for a method to determine the freestream density as accurately as possible.

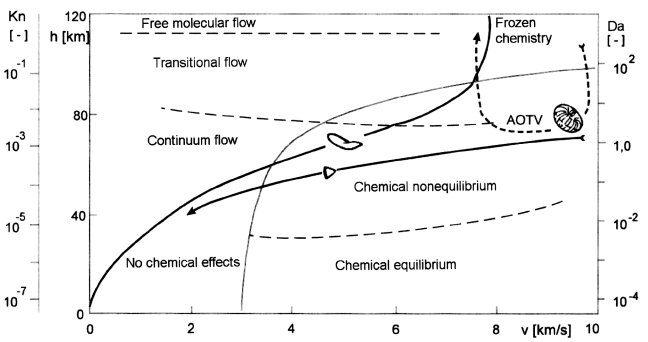

Fig. 2 Aerodynamic and kinetic flow regimes in the altitude-velocity map [8].

B. Numerical Approach to Determine the Freestream Density

It is evident that accurate knowledge of p_{t2}/q_∞ is essential for the accuracy of the entire ADS. The approaches described in Sec. II.A assume calorically perfect gas behavior. To investigate the correlation between the ratio p_{t2}/q_∞ and the flight parameters (u_∞, p_∞, ρ_∞) in detail, a numerical method is used to compute stagnation-point pressures p_{t2} from specified freestream conditions. High-temperature effects are allowed for assuming inviscid flow in thermochemical equilibrium. This keeps the method simple and applicable to any vehicle configuration without the need to specify its geometry as it would be necessary for a nonequilibrium flow model. Real-gas effects are modeled by curve-fit equations developed by Srinivasan et al. [5]. They are characterized by a broad and continuous range of validity as well as good accuracy.

From the mass, momentum, and energy conservation equations across a normal shock follows

$$p_2 = p_\infty + \rho_\infty u_\infty^2\left(1 - \frac{\rho_\infty}{\rho_2}\right) \tag{5}$$

and

$$h_2 = h_\infty + \frac{u_\infty^2}{2}\left[1 - \left(\frac{\rho_\infty}{\rho_2}\right)^2\right] \tag{6}$$

For given freestream conditions (u_∞, p_∞, ρ_∞) and an arbitrary starting value of ρ_2, the system of Eqs. (5) and (6) and

$$\rho_2 = \left(\frac{\tilde{\gamma}_2}{\tilde{\gamma}_2 - 1}\right)\frac{p_2}{h_2} \tag{7}$$

can be solved in an iterative manner using a curve-fit function

$$\tilde{\gamma} = \tilde{\gamma}(p, \rho) \tag{8}$$

where

$$\tilde{\gamma} := \frac{h}{e} \tag{9}$$

The relative change in the density value ρ_2 is calculated at the end of each iteration step,

$$\left|\frac{\rho_{2,\text{new}} - \rho_{2,\text{old}}}{\rho_{2,\text{old}}}\right| =: \varepsilon \tag{10}$$

where typical values of ϵ achieved a range from 10^{-7} to 10^{-4}. When the iteration process is completed, p_{t2} is calculated from the postshock quantities under the assumption of a compressible, calorically perfect gas. Considering only the postshock flow, this procedure does not lead to a significant deviation from the equilibrium flow model. This follows from the well-known fact that the pitot pressure is insensitive concerning high-temperature effects.

Atmospheric pressure $p_\infty(H)$ and density $\rho_\infty(H)$ have been chosen as input parameters to be specified for a certain number of altitudes ranging from $H = 90$ km to $H = 10$ km. These values are taken from the U.S. standard atmosphere. Thus, a two-dimensional altitude-velocity spectrum is computed for freestream velocities from $u_\infty = 400$ m/s up to 10,000 m/s. The results of this computation are illustrated in Fig. 3. For comparison, Fig. 4 shows the corresponding p_{t2}/q_∞ map for calorically perfect gas according to Eq. (2). As expected, the total deviation observed is not very large, but it is of importance when a highly accurate method for the determination of the freestream density is to be achieved.

Figure 5 shows a nominal shuttle trajectory as well as two comparative trajectories representing a high-lift ($m/A_{\text{ref}}C_L = 50$ kg/m^2) and a low-lift reentry ($m/A_{\text{ref}}C_L =$ 5000 kg/m^2). Figure 6 shows the differences between the results obtained from equilibrium gas computation, exact perfect-gas theory

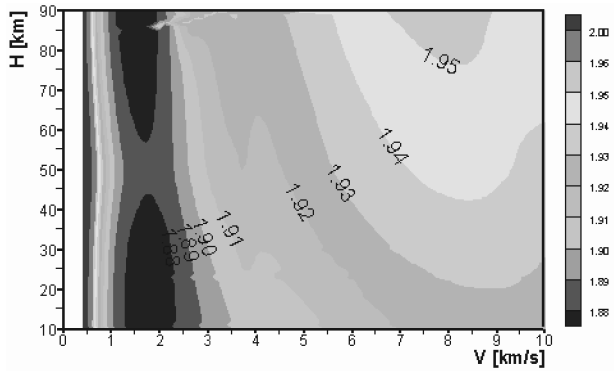

Fig. 3 p_{t2}/q_∞ distribution for standard-atmospheric conditions, equilibrium gas.

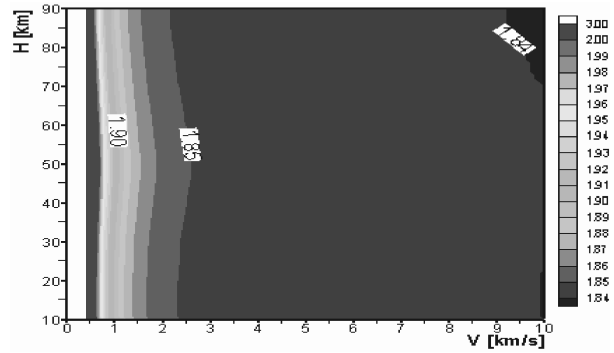

Fig. 4 p_{t2}/q_∞ distribution for standard-atmospheric conditions, calorically perfect gas, Eq. (2).

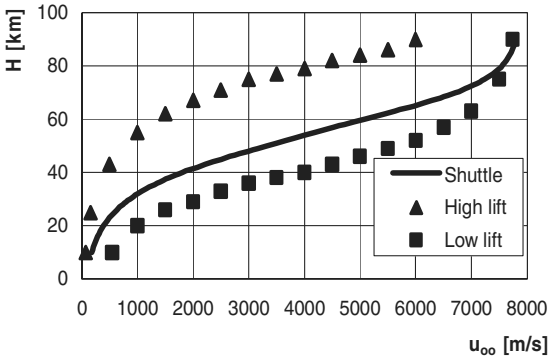

Fig. 5 Nominal and comparative trajectories.

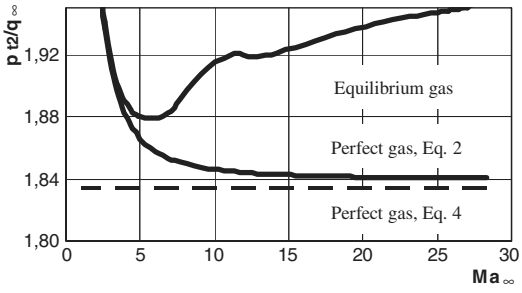

Fig. 6 Comparison of different gas assumptions: p_{t2}/q_∞ along nominal space shuttle entry trajectory.

[$\gamma_1 = \gamma_2 = 1.4$, Eq. (2)], and the approximation from Eq. (4) for the case of the space shuttle (STS) nominal reentry trajectory ($m/A_{\text{ref}}C_L = 550$ kg/m^2). It is evident from Fig. 6 that, particularly for the high Mach numbers relevant to reentry, the deviation between the perfect gas and equilibrium gas models is not negligible. According to the equilibrium gas model, the ratio p_{t2}/q_∞ approaches the value of 2 for high Mach numbers, which is in

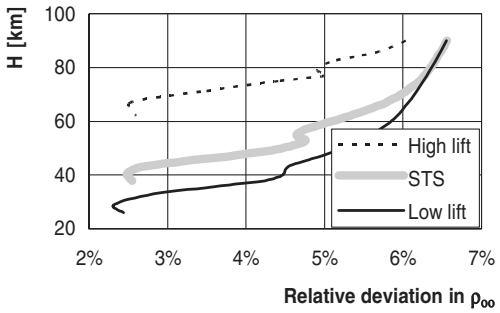

Fig. 7 Relative deviations in ρ_∞ between equilibrium and perfect gas as plotted versus altitude.

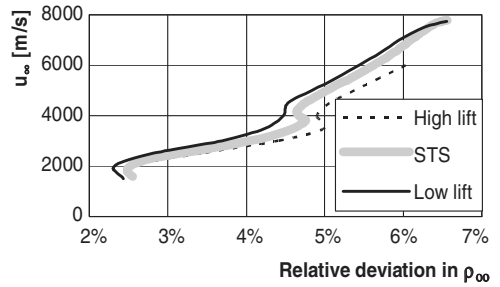

Fig. 8 Relative deviations in ρ_∞ between equilibrium and perfect gas as plotted versus velocity.

agreement with the ideal Newtonian theory; for the higher the flight Mach number, the smaller is the shock standoff distance and, thus, the more accurate is the Newtonian theory.

Figures 7 and 8 show the relative deviations in ρ_∞ or q_∞, provided the flight velocity is known from other measurements (GPS, etc.), between the equilibrium gas model and the perfect gas assumption of Eq. (4) as plotted versus altitude and flight velocity, respectively. As can be seen from a comparison of Figs. 7 and 8, the curves representing the three different trajectories of Fig. 5 roughly coincide when plotted versus the flight velocity. This is an important feature, which in the following allows one to reduce the number of independent variables. Figure 9 quantifies the remaining relative deviations in p_{t2}/q_∞ with respect to the space shuttle trajectory for high-lift and low-lift entry. Remarkably, for the entire range considered, from the low-lift up to the high-lift case the ratio p_{t2}/q_∞ appears to be predominantly dependent on the flight velocity u_∞, which leads to the following approach:

$$\frac{p_{t2}}{q_\infty} \approx f(u_\infty) \tag{11}$$

To determine the function $f(u_\infty)$) in Eq. (11) conveniently, that is, without using complex computer routines, a closed-form expression is required. Therefore, a curve-fit approximation to the equilibrium graph has been developed that yields $f = p_{t2}/q_\infty$ as a function of the flight velocity u_∞. The curve-fit function f is defined in a piecewise

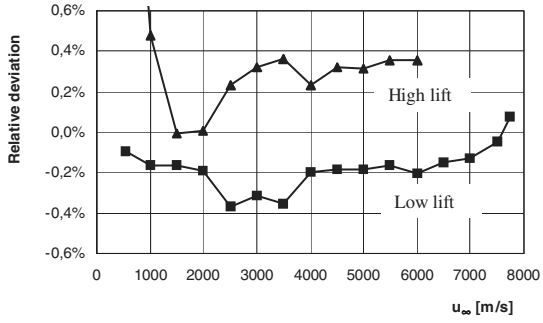

Fig. 9 Relative deviations in p_{t2}/q_∞ with respect to space shuttle nominal trajectory.

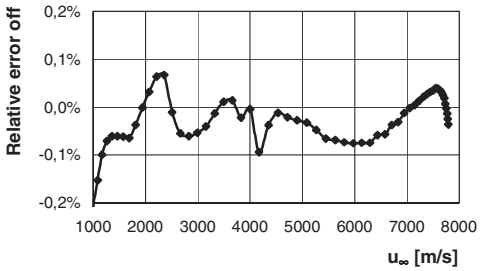

Fig. 10 Curve-fit accuracy for space shuttle nominal trajectory.

manner,

$$f = \begin{cases} f_1 & \text{for } 1000 \le u_\infty < 4170 \text{ m/s} \\ f_2 & \text{for } 4170 \le u_\infty \le 10,000 \text{ m/s} \end{cases} \tag{12}$$

where f_2 is linear and f_1 is a 16th-order polynomial function:

$$f_1(u_\infty) = a_1 + a_2 u_\infty + [a_3(u_{\infty-} - a_4)]^{16} + [a_5(u_\infty - a_6)]^6 - a_7(u_\infty - a_\infty)(u_\infty - a_9)(u_\infty - a_{10}) - a_{11} \tag{13}$$

$$f_2(u_\infty) = a_1 + a_2 u_\infty \tag{14}$$

where

$$a_1 = 1.875 \qquad a_2 = 10^{-5} \qquad a_3 = 0.00043 \qquad a_4 = 2600$$
$$a_5 = 0.0001 \qquad a_6 = 2600 \qquad a_7 = 10^{-11} \qquad a_8 = 1270$$
$$a_9 = 2828 \qquad a_{10} = 4172 \qquad a_{11} = 0.002$$

Note that f_2 has been extrapolated for up to 10,000 m/s. Figure 10 shows the deviation of the curve fit from the data of the space shuttle nominal trajectory.

A comparison of the curve-fit results with the entire altitude-velocity map, Fig. 3, results in a distribution of relative errors $\varepsilon_f(u_\infty, H)$ where

$$\varepsilon_f = \frac{f - (p_{t2}/q_\infty)}{p_{t2}/q_\infty} \tag{15}$$

and p_{t2}/q_∞ is determined from the actual freestream conditions by means of the equilibrium gas model. Because the approximate value f is used to calculate the freestream dynamic pressure q_∞, an error $\varepsilon_f \neq 0$ will result in an erroneous dynamic pressure and, thus, freestream density value. The relative error in the dynamic pressure, ε_q, is of a similar form as compared to ε_f:

$$\varepsilon_q = \frac{(p_{t2}/q_\infty) - f}{f} \tag{16}$$

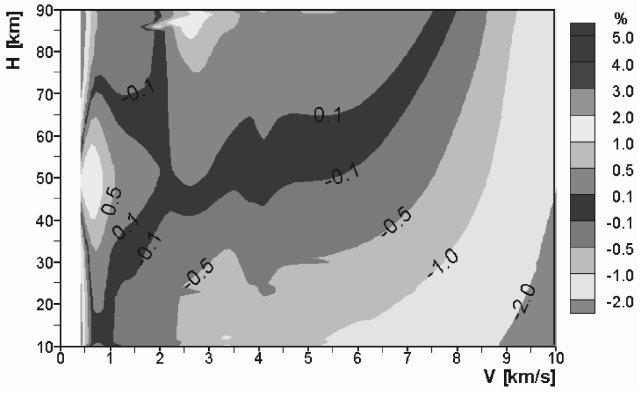

Fig. 11 Relative error ε_q, ρ_∞ (%) resulting from use of the curve fit $f(u_\infty)$.

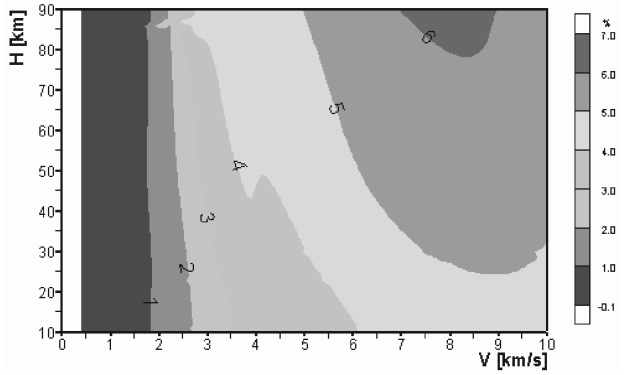

Fig. 12 Relative error in q_∞, ρ_∞ (%) for exact perfect-gas theory, Eq. (2).

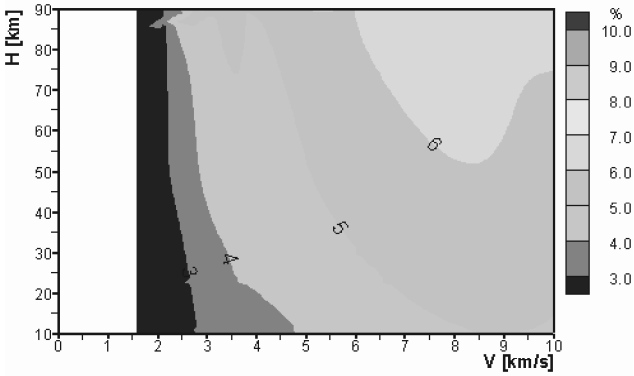

Fig. 13 Relative error in q_∞, ρ_∞ (%) according to approximation of Eq. (4).

The error distribution $\varepsilon_q(u_\infty, H)$ is presented in Fig. 11. For the purpose of comparison, the error estimation has also been applied to calorically perfect gas [Eq. (2)] as well as to the approximative method of Eq. (4); see Figs. 12 and 13. A comparison of Fig. 11 with Figs. 12 and 13 shows an increase in accuracy for the technique presented in the present paper. Errors are approximately 1 order of magnitude smaller than the conventionally obtained values, which range from 2 to 7% for the most part. Moreover, although the curve-fit function $f = f(u_\infty)$ has been constructed from a lifting reentry trajectory, an a posteriori consideration documents its applicability to almost the entire velocity/altitude regime considered, thus including ballistic entry and ascend trajectories. This becomes evident from Fig. 11, which documents that for the entire velocity/altitude regime investigated the maximum error in q_∞ or ρ_∞ does not exceed 2%.

C. Analytical Approach to Determine the Freestream Density

A second method to determine the freestream density from pitot-pressure measurements in high-enthalpy flows yields an analytically closed expression based on hypersonic theory. The continuity equation for a one-dimensional flow across a normal shock wave becomes

$$\rho_\infty u_\infty = \rho_{2E} u_{2E} \tag{17}$$

if thermochemical equilibrium is assumed on the stagnation streamline behind the shock, $(2) = (2E)$. Accordingly, the momentum equation becomes

$$p_\infty + \rho_\infty u_\infty^2 = p_{2E} + \rho_{2E} u_{2E}^2 \tag{18}$$

In such a flow, the postshock Mach number typically ranges between 0.2 and 0.3. As a first approximation, compressibility effects can thus be ignored ($\rho_{2E} \approx \rho_{t2}$), and Bernoulli's equation can be applied to determine the pitot pressure:

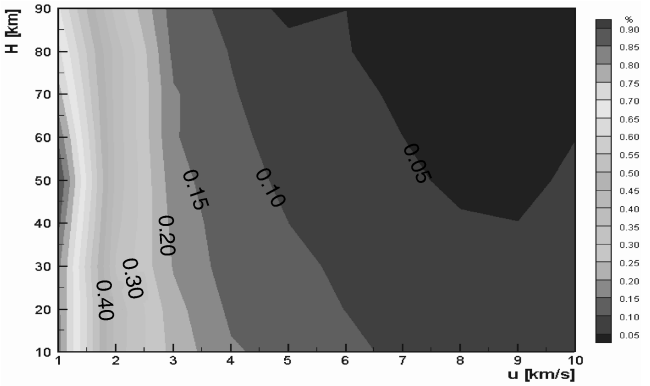

Fig. 14 Relative deviation of calculated atmospheric densities, Eq. (21), from standard-atmospheric freestream densities due to assumption, Eq. (19) (%).

$$p_{t2} = p_{2E} + \frac{\rho_{2E}}{2} u_{2E}^2 \tag{19}$$

Substituting Eqs. (17) and (19) into Eq. (18) yields a quadratic equation in ρ_∞,

$$p_\infty + \rho_\infty u_\infty^2 = p_{t2} + \frac{(\rho_\infty u_\infty)^2}{2\rho_{2E}} \tag{20}$$

Solving Eq. (20) yields

$$\rho_\infty = \rho_{2E}\left[1 - \sqrt{1 - \frac{2}{\rho_{2E} u_\infty^2}(p_{t2} - p_\infty)}\right] \tag{21}$$

where the postshock density is approximated by

$$\rho_{2E} \approx \rho_{t2}(h_{t2}, p_{t2}) \tag{22}$$

$$h_{t2} = \frac{u_\infty^2}{2} + c_p T_\infty \tag{23}$$

Hence, Eqs. (21–23) represent a method to compute atmospheric densities from pitot pressure and the freestream quantities velocity, temperature, and static pressure; the specific heat is nearly constant below 100 km altitude, $c_p = 1004$ J/kg. p_{t2} and u_∞ values are obtained from in-flight measurements whereas p_∞ and T_∞ can be estimated: these quantities have rather little influence on the result as $c_p T_\infty \ll u_\infty^2/2$ and $p_\infty \ll p_{t2}$. Hence, atmospheric fluctuation can be ignored, and standard-atmospheric values can be assumed. Also, the values may be roughly estimated if the altitude is unknown. Even setting the freestream pressure to $p_\infty = 0$ merely causes errors of 0.01–1% in the freestream density for velocities $u_\infty \geq 3$ km/s.

The error caused by using Bernoulli's equation (19) is visualized in Fig. 14. The density values ρ_∞ are calculated by means of Eq. (21) where ρ_{2E} and p_{t2} are determined from the given standard-atmospheric freestream conditions of the respective altitude using the computer routine described in Sec. II.B. Furthermore, the exact values of p_∞ of the model atmosphere considered are used. The small error values corroborate the theory of an incompressible postshock flow thus justifying the use of Eq. (19).

It is interesting to note that this procedure also allows one to determine the flight Mach number for a given flight velocity known from GPS or radar data. For this purpose, Eq. (20) is employed to deduce a more accurate value of the freestream pressure, where the required values of ρ_∞ and ρ_{2E} are known from the method described above:

$$p_\infty = p_{t2} - \frac{\rho_\infty u_\infty^2}{2}\left(2 - \frac{\rho_\infty}{\rho_{2E}}\right) \tag{24}$$

yielding the speed of sound

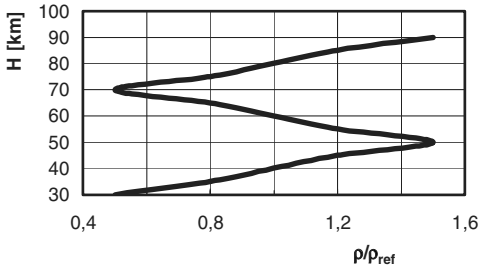

Fig. 15 Assumed deviation from standard-atmospheric density.

$$\alpha_\infty = \sqrt{\gamma \frac{p_\infty}{\rho_\infty}} \tag{25}$$

and, hence, the flight Mach number

$$Ma_\infty = \frac{u_\infty}{a_\infty} \tag{26}$$

D. Capability to Resolve Atmospheric Density Fluctuations

To investigate the accuracy under nonstandard conditions, the results for fluctuating densities have been compared. The space shuttle nominal reentry trajectory is used as a flight path; see Fig. 5. Atmospheric pressure is taken to show a standard distribution. Figure 15 shows an arbitrary density distribution compared to standard-atmospheric values (ρ_{ref}). In the following these density values are compared with those determined by the two methods described above. Using an arbitrarily defined model atmosphere for validation has the advantage that the input data are precisely known and that the data are thus free of any errors. In the case of applying the described method to real flight data and comparing the flight data derived density values with those achieved by the present method would not allow for a clear statement on the accuracy of the procedure described in this paper. Because in this case the difference of the flight data from the derived data would not only result from the approximations in the theoretical model but also from the flight measurement uncertainties, which are not known or not known precisely enough. So it would not be possible to separate the different sources of error. Even in the case of full agreement between flight data and theoretical data, this could not lead to a statement on the accuracy of the method, because it is most probable that in this case flight measurement errors and errors of the theoretical model just compensate.

Figure 16 shows the corresponding relative errors according to the curve-fit method [Eqs. (11–14)] and the analytical approach [Eqs. (21–23)]. Flight values of u_∞ and computer-derived equilibrium values of p_{t2} for the actual freestream conditions are used in default of measurement results. For the application of Eq. (21), ρ_{2E} is determined according to Eqs. (22) and (23). The freestream quantities p_∞ and T_∞ are approximated by means of the U.S. standard atmosphere. Even under extreme conditions, both methods exhibit good results with relative errors of less than 0.3% for $Ma_\infty > 5$ or $H > 40$ km, respectively.

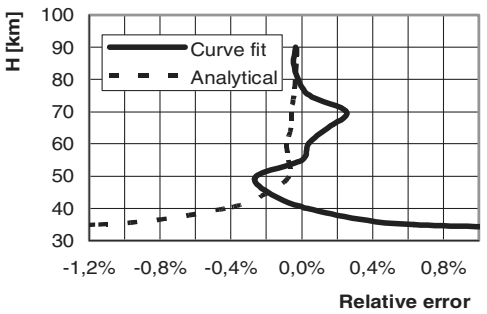

Fig. 16 Relative error in predicted density for density distribution given in Fig. 15.

III. Conclusions

To date, most of the air data systems are based on the assumption of perfect-gas behavior causing errors of 2–7%, determining the freestream density under the assumption of a known flight velocity. In this paper, two methods have been presented to determine the atmospheric density from in-flight pitot-pressure and flight-velocity measurements. These are a numerically obtained curve-fit method as well as an analytically derived function, both applicable to continuum flow. The investigated flight regime covers altitudes between $H = 10$ km and $H = 90$ km and velocities of up to 10 km/s. Equation (21) represents an analytically derived correlation between ρ_∞, p_∞, u_∞, p_{t2}, and ρ_{2E} that clearly shows the influence of the individual quantities. To calculate ρ_∞ conveniently for many different conditions, however, it is necessary to use a computer routine that computes ρ_{2E} according to Eq. (22). The curve-fit method [Eqs. (11–14)], on the other hand, represents a numerically derived expression. However, it yields direct results without further use of any computer routine. Both approaches allow for high-temperature equilibrium effects thus achieving significantly increased accuracies. The results show marginal errors of less than 0.5% for trajectories relevant to reentry, independently of any atmospheric fluctuations.

Possible sources of error are viscous and nonequilibrium effects as well as radiation. Both methods assume thermochemical equilibrium in the stagnation region and negligible radiative losses in the shock layer. By limiting the investigated flight regime to freestream velocities $u_\infty \leq 10$ km/s and altitudes $H \leq 90$ km, these assumptions are justifiable. To investigate the influence of nonequilibrium effects, Navier–Stokes computations of the flow around a cylinder have been performed for chemical nonequilibrium. These first computations show that, for the same pitot pressure, the freestream density value obtained by means of the present method and that from a nonequilibrium flow model only deviate by less than 1% demonstrating the small influence of nonequilibrium effects on the method presented. This is not surprising, because the two methods presented are based on the pitot pressure, the insensitivity of which concerning a nonequilibrium shock layer flow is very well known. Another source of errors may be due to viscous effects in the stagnation region. According to Williams [6], the stagnation-point pressure p_{t2} in the flow over a spherically tipped body increases significantly for low Reynolds numbers $Re_d < 10^2$ (*Barker effect*) whereas this influence remains small for $Re_d < 10^2$ (d: diameter of the sphere). Hence, the flow along the stagnation streamline of a sphere with diameter $d \geq 1$ m, for instance, is not subject to significant viscous effects within the lower 90 km of the atmosphere for velocities $u_\infty > 0.5$ km/s.

In summary, the two methods presented are simple but of high accuracy. Their simplicity results in very short computing times, which makes them suitable for an online data reduction during reentry, providing data, for example, for flight control loops.

References

[1] Enzian, A., Devezeaux, D., Mohamed, A., Thivet, F., Tran, P., and Tribot, J.-P., "Flight Experiments to Address Unsolved Aerothermodynamic Issues for a Future European Reusable Space Launcher," *Aerothermodynamics for Space Vehicles*, ESA SP-487, European Space Agency, Noordwijk, The Netherlands, Feb. 2002, pp. 451–455.

[2] Koppenwallner, G., and Müller-Eigner, R., "Definitionsstudie Anström- und Oberflächenflusssonden für den verdünnten Strömungsbereich, Teil 2: Staudrucksonde," Rept. No. 92-15, HTG Hyperschalltechnologie Göttingen, Germany, 1992.

[3] Müller-Eigner, R., Koppenwallner, G., and Fritsche, B., "Pressure and Heat Flux Measurement with RAFLEX II During MIRKA Re-Entry," *Third European Symposium on Aerothermodynamics for Space Vehicles*, ESA SP-426, European Space Agency, Noordwijk, The Netherlands, Jan. 1999, pp. 685–694.

[4] Anderson, J. D., *Hypersonic and High Temperature Gas Dynamics*, McGraw–Hill, New York, 1989.

[5] Srinivasan, S., Tannehill, J. C., and Weilmuenster, K. J., "Simplified Curve Fits for the Thermodynamic Properties of Equilibrium Air," NASA RP1181, 1987.

[6] Williams III, J. C., "Rise of Total Pressure Near the Stagnation Point on a Sphere," *AIAA Journal*, Vol. 40, No. 3, 2002, pp. 576–579.

[7] Talay, T. A., White, N. H., and Naftel, J. C., "Impact of Atmospheric Uncertainties and Viscous Interaction Effects on the Performance of Aeroassisted Orbital Transfer Vehicles," *Thermal Design of Aeroassisted Orbital Transfer Vehicles*, edited by H. F. Nelson, Vol. 96, Progress in Astronautics and Aeronautics, AIAA, New York, 1985, pp. 198–229.

[8] Messerschmid, E., and Fasoulas, S., *Raumfahrtsysteme*, Springer–Verlag, Berlin, 2000, p. 394.

A. Ketsdever
Associate Editor